

Implementation of Perdew-Zunger self-interaction correction in real space using Fermi-Löwdin orbitals

Carlos M. Diaz,^{1, a)} Phanish Suryanarayana,² Qimen Xu,² Tunna Baruah,¹ John Pask,³ and Rajendra Zope¹

¹⁾*Department of Physics, University of Texas at El Paso, El Paso, Texas 79968, USA*

²⁾*College of Engineering, Georgia Institute of Technology, Atlanta, GA 30332, USA*

³⁾*Physics Division, Lawrence Livermore National Laboratory, Livermore, CA 94550, USA*

(Dated: 4 August 2021)

Most widely used density functional approximations suffer from self-interaction (SI) error, which can be corrected using the Perdew-Zunger (PZ) self-interaction correction (SIC). We implement the recently proposed size-extensive formulation of PZ-SIC using Fermi-Löwdin Orbitals (FLOs) in real space, which is amenable to systematic convergence and large-scale parallelization. We verify the new formulation within the generalized Slater scheme by computing atomization energies and ionization potentials of selected molecules and comparing to those obtained by existing FLOSIC implementations in Gaussian based codes. The results show good agreement between the two formulations, with new real-space results somewhat closer to experiment on average for the systems considered. We also obtain the ionization potentials and atomization energies by scaling down the Slater statistical average of SIC potentials. The results show that scaling down the average SIC potential improves both atomization energies and ionization potentials, bringing them closer to experiment. Finally, we verify the present formulation by calculating the barrier heights of chemical reactions in the BH6 dataset, where significant improvements are obtained relative to Gaussian based FLOSIC results.

I. INTRODUCTION

The Kohn-Sham (KS) formulation of the density functional theory (DFT) has emerged as a standard method for electronic structure calculations of atoms, molecules, and solids.¹ It is among the most widely used quantum mechanical methods for the study of electronic properties of solids. The many-electron effects in the KS theory are incorporated into the exchange-correlation functional, the exact form of which is currently unknown. Practical applications of KS-DFT therefore employ an approximation to the exchange-correlation functional, the accuracy of which determines the fidelity of the simulation. Since there is no systematic way to construct the exchange-correlation functional, a large number of approximations have been proposed.^{2,3} Both exchange and correlation are generally approximated together to obtain systematic error cancellation. One way of constructing functionals, pursued by Perdew and coworkers, is by considering the known physical properties of the exact exchange-correlation functional and other exact properties.^{2,4,5} Such functionals, classified as non-empirical, typically show greater predictive capability than functionals empirically fitted to databases of various chemical properties.

Perdew and Schmidt² have classified exchange-correlation functionals using an analogy to Jacob's ladder wherein more sophisticated density functional approximations (DFA) correspond to higher rungs on the ladder. The celebrated local spin density approximation (LSDA) functional,^{6,7} which depends only on the electron density, belongs to the first rung of the ladder. This functional has been used for decades to study electronic structure related properties in solid state physics. Semi-local functionals such as the generalized gradient approximation (GGA) depend on the electron density

and its gradients, while meta-GGA functionals additionally depend on the Laplacian of the density or kinetic-energy density. These functionals belong to the second and third rungs, respectively. The higher rungs' functionals include a certain percent of non-local Hartree-Fock exchange along with DFAs.^{2,3} Acceptable accuracy of the available functionals along with efficient implementation of KS formulations in several easy-to-use codes have resulted in explosive growth of KS-DFT applications.

The LSDA and semi-local functionals often describe equilibrium properties sufficiently accurately but fail to provide accurate results for reaction barrier heights in chemical reactions where the bonds between atoms are stretched.⁸ In fact, these functionals also fail to describe one electron systems accurately, which has been attributed to the self-interaction error (SIE) of these functionals.⁸ Specifically, in the case of a one electron system, the exact exchange-correlation energy cancels the Coulomb energy. However, this cancellation is incomplete in approximate functionals, and residual self-interaction remains. A number of approaches have been proposed to remove the SIEs.^{7,9-16} In this work, we focus on the most widely used self-interaction-correction, developed by Perdew and Zunger (PZ-SIC)⁷, which has been used to study atoms, molecules, and solids.^{8,13,14,17-67}

A. Perdew-Zunger Self-interaction-correction (PZ-SIC)

In 1981, Perdew-Zunger (PZ) provided a definition of one-electron SIE and outlined a procedure to eliminate this error from the DFAs.⁷ In the PZ approach, the SIE is removed on an orbital by orbital basis according to the following equation:

$$E^{SIC} = - \sum_{i\sigma}^{N_{occ}} (U[\rho_{i\sigma}] + E_{xc}^{DFA}[\rho_{i\sigma}, 0]). \quad (1)$$

^{a)}Electronic mail: cmdiaz6@miners.utep.edu

Here, $U[\rho_{i\sigma}]$ and $E_{xc}^{DFA}[\rho_{i\sigma}, 0]$ are the Coulomb and exchange-correlation energy of the i^{th} occupied orbital, σ is the spin index and N_{occ} is the number of occupied orbitals. The orbital electron density, $\rho_{i\sigma} = |\psi_{i\sigma}|^2$, where the $\psi_{i\sigma}$ are the KS orbitals. The above corrections make the DFA exact for any one-electron density. The correction should vanish for the exact functional. The SIC method of Perdew-Zunger satisfies this criterion. The total energy with the PZ-SIC method is given by

$$E = E^{KS} + E^{SIC}, \quad (2)$$

where,

$$E^{KS} = \sum_{i\sigma} f_{i\sigma} \langle \psi_{i\sigma} | -\frac{\nabla^2}{2} | \psi_{i\sigma} \rangle + \int d^3r \rho(\vec{r}) v_{ext}(\vec{r}) + \frac{1}{2} \iint d^3r d^3r' \frac{\rho(\vec{r})\rho(\vec{r}')}{|\vec{r}-\vec{r}'|} + E_{xc}[\rho_{\uparrow}, \rho_{\downarrow}]. \quad (3)$$

Here, v_{ext} is the external potential. The electron density, $\rho = \rho_{\uparrow} + \rho_{\downarrow} = \sum_{\sigma} \rho_{\sigma} = \sum_{i,\sigma} f_{i\sigma} |\psi_{i\sigma}|^2$. $f_{i\sigma}$ is the occupation of the $\psi_{i\sigma}$ orbital.

The variational minimization of the above energy functional results in a set of orbital dependent PZ-SIC equations:

$$\left[-\frac{\nabla^2}{2} + v_{eff}^{i\sigma}(\vec{r}) \right] \psi_{i\sigma} = \hat{H}_{i\sigma}^{PZ-SIC} \psi_{i\sigma} = \sum_{j=1, \sigma}^N \lambda_{ji}^{\sigma} \psi_{j\sigma}. \quad (4)$$

Here,

$$v_{eff}^{i\sigma}(\vec{r}) = v_{ext}(\vec{r}) + \int d^3r' \frac{\rho(\vec{r}')}{|\vec{r}-\vec{r}'|} + v_{xc}^{\sigma}(\vec{r}) - \left\{ \int d^3r' \frac{\rho_{i\sigma}(\vec{r}')}{|\vec{r}-\vec{r}'|} + v_{xc}^{i\sigma}(\vec{r}) \right\}. \quad (5)$$

The first term $v_{ext}(\vec{r})$ in above equation is the external potential, the second term is the Coulomb potential due to the electrons, and v_{xc} is the exchange-correlation potential (of DFA). The last two terms enclosed in the curly bracket correspond to the orbital SIC potential $V_{i\sigma}^{SIC}$, composed of the self-Coulomb and self-exchange-correlation potential. Note that, unlike the standard KS equations, the effective potential in Eq. (4) is orbital dependent. The matrix of Lagrange multipliers $\lambda_{ij} = \langle \psi_{i\sigma} | \hat{H}_{i\sigma}^{PZ-SIC} | \psi_{j\sigma} \rangle$ is introduced in Eq. 4 to ensure the orthogonality of occupied N orbitals of spin σ . At the minimum of the PZ-SIC energy, the non-Hermitian Lagrange multiplier matrix becomes Hermitian. Thus, the orbitals minimizing the Hamiltonian in Eq. 4 satisfy Pederson's localization equations^{18,19} $\lambda_{ji}^{\sigma} = \lambda_{ij}^{\sigma}$. Some implementations³⁰ of PZ-SIC method enforce satisfaction of *localization equations*, a method which results in additional computational effort. The orthogonal orbitals that satisfy the localization equations are localized orbitals. Various localized orbitals such as Foster-Boys⁶⁸ and Pipek-Mezey⁶⁹, for example, have been used in solving the PZ-SIC scheme.^{8,20,23} These are related to Kohn-Sham orbitals by unitary transformation. In 2014, Pederson and coworkers⁷⁰ used Fermi-Löwdin orbitals⁷¹⁻⁷³ in the PZ-SIC scheme. Below we describe in brief the details of that approach.

B. Fermi-Löwdin orbitals SIC (FLOSIC)

Recently, Pederson, Ruzsinszky, and Perdew⁷⁰ introduced the unitarily invariant implementation of PZ-SIC using Fermi-Löwdin orbitals (FLOSIC).^{72,73} FLOSIC makes use of localized Fermi orbitals (FOs) $F_{i\sigma}$ which are defined by the transformation of KS orbitals as

$$F_{i\sigma}(\vec{r}) = \frac{\sum_{\alpha} \psi_{\alpha\sigma}^*(\vec{a}_{i\sigma}) \psi_{\alpha\sigma}(\vec{r})}{\sqrt{\sum_{\alpha} |\psi_{\alpha\sigma}(\vec{a}_{i\sigma})|^2}}. \quad (6)$$

Here, $\vec{a}_{i\sigma}$ are points in space called Fermi-orbital descriptors (FODs). Neglecting the spin index, the above equation can be rewritten as

$$F_i(\vec{r}) = \sum_{\alpha}^{N_{occ}} F_{i\alpha} \psi_{\alpha} = \frac{\rho(\vec{a}_i, \vec{r})}{\sqrt{\rho(\vec{a}_i)}}, \quad (7)$$

where the transformation matrix $F_{i\alpha}$ is defined as

$$F_{i\alpha} = \frac{\psi_{\alpha}^*(\vec{a}_i)}{\sqrt{\rho(\vec{a}_i)}}. \quad (8)$$

The FOs are normalized but not orthogonal, so they are orthogonalized using Löwdin orthogonalization method to generate the Fermi-Löwdin orbitals (FLOs) $\phi_{i\sigma}$. The FLOs depend on the FOD positions. The change of FOD positions thereby alters the total energy. The optimal FOD positions are obtained by minimizing the self-consistent SIC energy using the FOD forces^{74,75} as follows

$$\frac{dE^{SIC}}{da_m} = \sum_{kl} \epsilon_{kl}^k \left\{ \left\langle \frac{d\phi_k}{da_m} | \phi_l \right\rangle - \left\langle \frac{d\phi_l}{da_m} | \phi_k \right\rangle \right\}. \quad (9)$$

The derivatives $\langle (d\phi_k)/(da_m) | \phi_l \rangle$ require evaluating $\langle (dF_k)/(da_m) \rangle$ which can be accomplished using following relations,

$$\nabla_{a_i} F_i(\vec{r}) = \sum_{\alpha} \{ \nabla_{\vec{a}_i} F_{i\alpha} \} \psi_{\alpha}(\vec{r}) \quad (10)$$

$$\nabla_{a_i} F_{i\alpha} = F_{i\alpha} \left\{ \frac{\nabla_{a_i} \psi_{\alpha}(\vec{a}_i)}{\psi_{\alpha}(\vec{a}_i)} - \frac{\nabla_{a_i} \rho(\vec{a}_i)}{2\rho(\vec{a}_i)} \right\} \quad (11)$$

The FLOSIC approach described above, unlike the traditional PZ-SIC implementations, requires optimizing the N positions or $3N$ parameters of FODs and has formally lower cost than the traditional PZ-SIC implementation which requires obtaining N^2 coefficients to satisfy the localization equations. The FLOSIC method has been implemented in Gaussian-orbital-based packages and has been successfully applied to study a wide array of electronic properties.^{15,16,44,57-60,62-67,76-79}

In this work, we present a formulation and implementation of the FLOSIC method in real space. The real-space formulation enables rigorous, systematic convergence for all atomic species and configurations as well as large-scale parallelism to reach larger length and time scales than previously accessible at this level of theory. While the PZ-SIC method using Kohn-Sham orbitals has been implemented in real space

previously^{41,42,50,51,53,54,80} we present the first implementation of the FLOSIC method, to our knowledge. In Sec. II, we present the details of the formulation and implementation. To demonstrate and verify the formulation and implementation, we compute the atomization energies, barrier heights, and ionization potentials of selected molecules and compare to previous results obtained by standard Gaussian based codes and experiment. Computational details and results are presented in Secs. III and IV, respectively.

II. REAL-SPACE FORMULATION AND IMPLEMENTATION

A. M-SPARC code base

To facilitate rapid implementation and testing, we formulate and implement the self-interaction correction in real space in the M-SPARC prototype code,⁸¹ a serial implementation of the massively parallel SPARC real-space electronic structure code,^{82–84} sharing the same structure, algorithms, input, and output.

M-SPARC is an open-source software package that can perform Kohn-Sham DFT calculations for isolated systems such as molecules as well as extended systems such as crystals and surfaces. M-SPARC employs the pseudopotential approximation⁸⁵ to facilitate the efficient solution of the Kohn-Sham equations for all elements in the periodic table. In addition, it employs a local real-space formulation for the electrostatics,^{86–88} wherein the electrostatic potential — sum of ionic and Hartree potentials — is obtained via the solution of a Poisson equation. In this framework, M-SPARC performs a uniform real-space discretization of the Kohn-Sham and Poisson equations, using a high-order centered finite-difference approximation for differential operators and the trapezoidal rule for integral operators.

M-SPARC employs the self-consistent field (SCF) method⁸⁵ to solve for the electronic ground state. The superposition of isolated-atom electron densities is used as the initial guess for the first SCF iteration in the simulation, whereas for every subsequent atomic configuration encountered, extrapolation based on previous configurations’ solutions is employed.⁸⁹ The SCF method is accelerated using the restarted variant⁹⁰ of Periodic Pulay mixing⁹¹ with real-space preconditioning.⁹² For spin polarized calculations, mixing is performed simultaneously on both components.

In every SCF iteration, M-SPARC performs a partial diagonalization of the linear eigenproblem using the CheFSI method,^{93,94} with multiple Chebyshev filtering steps performed in the first SCF iteration of the simulation⁹⁵. While performing the Hamiltonian-matrix products, the Kronecker product formulation for the Laplacian is used,⁹⁶ and the remaining terms are handled in a matrix-free fashion with zero-Dirichlet or Bloch-periodic boundary conditions prescribed on the orbitals along directions in which the system is finite or extended, respectively. The electrostatic potential is determined by using the AAR linear solver^{97,98} for solving the Poisson equation. Laplacian-vector products are

performed using the Kronecker product formulation,⁹⁶ with Dirichlet/periodic boundary conditions prescribed along directions in which the system is finite or extended, respectively. In particular, Dirichlet values are determined using a multipole expansion for isolated systems and a dipole correction for surfaces and nanowires.^{99,100}

M-SPARC thus provides a natural framework to implement the FLOSIC self-interaction correction in real space, for both isolated and periodic systems. Its extension to SPARC should be relatively straightforward, providing large-scale parallelism for performing such calculations.

B. Interpolation Scheme: Transformation matrix and FOD forces

In order to construct the transformation matrix F_{ij} (Eq. (8)) the wavefunction $\psi(\vec{a}_i)$ needs to be evaluated at the FOD position \vec{a}_i , which can fall between grid points. In such case, values between grid points are obtained by cubic interpolation of values on the grid. The density $\rho(\vec{a}_i)$ is then constructed as $\rho(\vec{a}_i) = \sum_j^N f_j |\psi_j(\vec{a}_i)|^2$, where f_j is the occupancy of the j -th state. Currently all calculations use a fixed integer occupation. Calculating the forces on FODs according to Eq. (9) also requires the gradients $\nabla\psi(\vec{a}_i)$ at the FOD positions \vec{a}_i . We first obtain the gradient at each grid point using the 1st-order central-difference approximation for all central points, and forward- and backwards-difference at the edges. The gradients $\nabla\psi(\vec{a}_i)$ are then obtained by cubic interpolation as for the transformation matrix, F . Proceeding in this way, forces and energy minima were found to coincide well. For Li_2 , analytic FOD forces differed by $2.6 \times 10^{-6} E_h/\text{Bohr}$ at equilibrium when compared against finite-difference force calculations using a spacing of 10^{-2} Bohr.

C. Self-consistency

The development of full self-consistency in FLOSIC was shown to lower energies for certain systems.¹⁰¹ In their work, Yang *et al.* employed an iterative approach to solve Eq. (4) using Jacobi rotations ($\text{SC}_{\text{Jacobi}}$).

In this approach, an approximate Hamiltonian matrix is first constructed as

$$\tilde{H}_{m\sigma} = \langle \phi_{m\sigma} | \hat{H}_\sigma^{KS} + V_{m\sigma}^{SIC} | \phi_{n\sigma} \rangle \quad (12)$$

where \hat{H}_σ^{KS} is the traditional KS Hamiltonian. The FLOs and the unoccupied virtual orbitals are made orthogonal through pairwise Jacobi rotations which are carried out iteratively until the matrix elements for \tilde{H} between the occupied ϕ_i and virtual orbitals ϕ_j vanishes.

An alternative approach has since been introduced which uses the Unified Hamiltonian described by Heaton, Harrison, and Lin¹⁷ (SC_{UH}). In both cases, operations are performed on the full Hamiltonian of size N_b^2 , where N_b is the number of basis functions in the calculation. In the finite-difference methodology, the Hamiltonian is of order N_{grid}^2 , where N_{grid} is the total number of grid points used in the calculation as

determined by the domain size and grid spacing. The size of the real-space Hamiltonian would quickly make these approaches prohibitively expensive. One approach to address this would be to employ discrete discontinuous basis projection (DDBP)¹⁰² to reduce Hamiltonian and orbital dimensions to a few tens per atom.

In the present work we use a simplified single Hamiltonian which is obtained by statistical average of the orbital dependent SIC potentials¹⁰³ (SC_{AvgSIC}). This eliminates the dependence on the full N_b^2 matrix elements. Thus the Hamiltonian used in the present work is given by

$$\hat{H} = -\frac{\nabla^2}{2} + v_{ext}(\vec{r}) + \int d^3r' \frac{\rho(\vec{r}')}{|\vec{r}-\vec{r}'|} + v_{xc}^\sigma(\vec{r}) + \frac{\sum_i^{N_{occ}} V_{i\sigma}^{SIC}(\vec{r}) \tilde{\rho}_{i\sigma}(\vec{r})}{\rho_\sigma(\vec{r})}. \quad (13)$$

Here, $\tilde{\rho}_{i\sigma}(\vec{r}) = |\phi_{i\sigma}(\vec{r})|^2$ is the FLO density, and $\rho_\sigma(\vec{r})$ is the spin electron density. Figure 1 illustrates the SCF procedure utilizing this approach. This approach resembles the traditional Slater average method but differs in two key respects. Firstly, the averaged potentials contain both the exchange and correlation components. Secondly, the average potential is constructed from orbital dependent potentials that are determined using the localized Fermi-Löwdin orbital densities and not the canonical (delocalized) Kohn-Sham orbital densities. Similarly, the weights $\tilde{\rho}_i$ used in averaging are also FLO densities. Such an approach using non-KS orbitals has been referred to by Messud and coworkers as a *generalized Slater* scheme.^{51,104} The difference from previous works is the use of Fermi-Löwdin orbitals in the present work. We note that the average Slater potential is a further approximation of the Krieger-Li-Iafrate approximation³⁶ to the optimized effective potential (OEP) where orbital-dependant shifts are ignored. Messud *et al.*¹⁰⁴ have noted that the generalized Slater scheme provides a significant improvement compared to the traditional SIC-Slater and Krieger-Li-Iafrate formalisms using canonical Kohn-Sham orbitals. A number of studies have emphasized the need for localized orbitals in PZSIC calculations on molecules and solids^{8,18–20,23,41,105} since, as mentioned earlier, canonical orbitals give vanishing correction for extended systems. An added benefit of having a single effective potential is that the SI-corrected unoccupied orbitals are available in this approximation.

We have also experimented with scaling the average SIC potential; Jónsson and coworkers have found such a scaled SIC to be more accurate in some cases when used with GGA functionals.¹⁰⁶

III. COMPUTATIONAL DETAILS

Total energies in M-SPARC calculations were converged to $10^{-3}E_h$ with respect to grid spacing and domain size. Optimized Norm-Conserving Vanderbilt (ONCV) pseudopotentials¹⁰⁷ were generated with exchange-correlation in the local density approximation (LDA)⁷ based on corresponding GGA¹⁰⁸ potentials in the SG15 library.¹⁰⁹

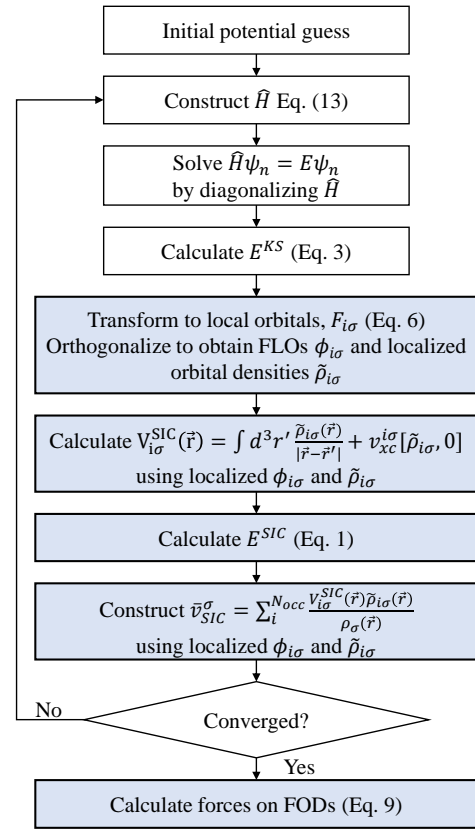


FIG. 1. Self-consistent FLOSIC procedure using the averaged SIC potential scheme for a given set of FODs. Steps making use of localized FLOs are indicated by color and greater width.

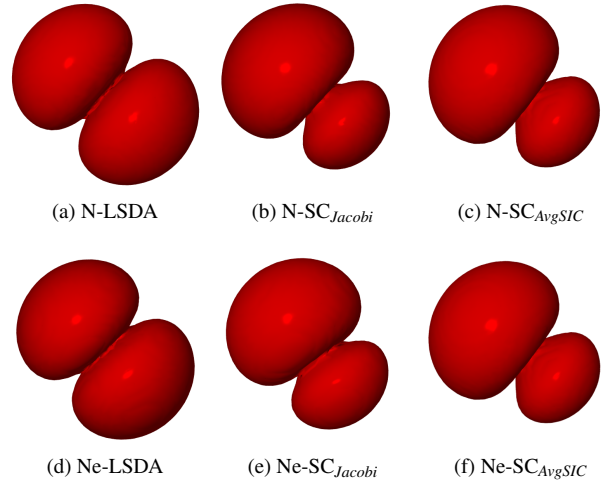


FIG. 2. The isosurface of p orbitals for (a) N and (d) Ne atoms (within LSDA). Likewise, the middle [(b) and (e)] and the right panel [(c) and (f)] show isosurfaces for N and Ne atoms sp hybridized orbitals in the SC_{Jacobi} (obtained using the FLOSIC code) and SC_{AvgSIC} (present work) methods.

The ONCV formulation employs multiple nonlocal projectors in each angular momentum channel to obtain high transferability across species, configurations, and external conditions. All calculations were tested using LSDA exchange and the PW92 correlation functional.

The FLOSIC code is an implementation based on the UTEP-NRLMOL code. The code uses an accurate numerical integration grid scheme.¹¹⁰ The default basis set¹¹¹ is shown to give comparable results to the cc-pVQZ basis set.⁴⁴ Calculations were also performed using the PyFLOSIC code¹¹², a pySCF¹¹³ based code, to produce benchmark calculations for comparison as it allows using basis sets with higher angular momentum functions. Non-self-consistent one-shot (OS) calculations were performed by calculating SIC energies at the end of a standard DFT calculation using the converged Kohn-Sham orbitals. Self-consistent (SC) calculations with the M-SPARC and FLOSIC codes employed the SC_{AvgSIC} potential approach described in Sec. II C. FLOSIC and PyFLOSIC calculations employed SC_{Jacobi} and SC_{UH} approaches as well. The starting FOD positions used in M-SPARC were optimized FOD positions from the FLOSIC code using BHS pseudopotentials. The FOD positions were further adjusted according to the forces as needed. All FODs were converged to a maximum force of $10^{-3} E_h/\text{Bohr}$. In the sections below we present results of our real-space formulation for atomic energies, atomization energies, ionization potentials and barrier heights, with comparisons to standard Gaussian based results.

IV. RESULTS

A. Basis set completeness

The real-space methodology discretizes the Kohn-Sham equations in a chosen domain on a uniform grid in real space. For periodic systems, the computational domain is the unit cell, while for isolated systems it is a box sufficiently large to contain the wavefunction tails to desired accuracy. Thus, for atomic and molecular systems of any species and configuration, discretization errors can be reduced as far as desired by refining the grid and increasing domain size. In the present calculations, grid and domain errors were converged to $10^{-3} E_h$ or less in all cases.

The systematic convergence afforded by real-space methods offers some advantages in the context of FLOSIC and other such advanced exchange-correlation formulations. In particular, since individual orbital densities vary more rapidly than the total density, higher resolution is generally required in FLOSIC calculations than for standard LDA and GGA; and this is readily obtained by refining the grid. In addition, where far-from-equilibrium configurations are of interest, such as for significantly stretched or compressed bonds, errors are again straightforwardly reduced as far as desired by simply refining the grid, in contrast to basis-set oriented approaches.

The FLOSIC and PyFLOSIC codes employ several basis sets to facilitate accurate calculations of a wide variety of properties. In addition to the default NRLMOL basis employed in the FLOSIC code, we also employed $pc-n$ basis

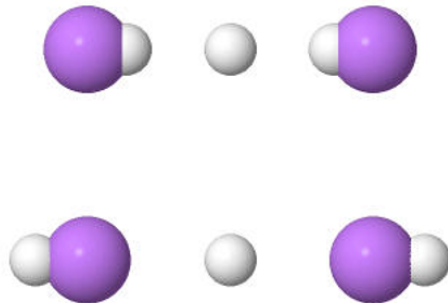


FIG. 3. Two sets of FODs for Li_2 each at different energy minima. The Li atoms (purple) and FODs (white) are shown.

sets,¹¹⁴ where $n = 0 - 4$, which have been designed to systematically converge to the basis set limit as n is increased. At the $pc-3$ and $pc-4$ levels, the basis for lithium makes use of f or higher angular momentum functions. As the FLOSIC code does not currently support f or higher angular momentum functions, the $pc-3$ and $pc-4$ results were obtained using PyFLOSIC.

B. Atoms

The hydrogen atom is the simplest system. For one electron systems, the PZ-SIC is exact. For the hydrogen atom a single FOD is required. The SIC energy in this case is independent of the FOD position. We find OS-SIC calculations differ by $0.12 mE_h$ among all implementations. Self-consistency improves the energies to within $0.016-0.36 mE_h$ of the exact answer ($0.5 E_h$). By refining the grid spacing to 0.2 Bohr , the self-consistent M-SPARC calculation comes within $0.016 mE_h$ of the exact energy. Using the $pc-2$ basis set, the LSDA and OS-SIC calculations effectively give the same energy between the FLOSIC code and PyFLOSIC. Self-consistency increases the difference by $0.3 mE_h$. This difference may be explained by the different implementations of self-consistency in each code, as detailed in Sec. II C. When the SIC equations are solved using the localization equations, it was found that s and p orbitals are hybridized into four symmetrically equivalent orbitals. Using the Slater-averaging approach to self-consistency we find the same hybridization as shown in Fig. 2.

Figure 2 shows the isosurfaces of p orbital densities of the nitrogen and neon atom obtained with standard LSDA calculations along with those obtained from the FLOSIC code, which uses Jacobi rotations to build the SIC Hamiltonian, and the present implementation, which uses a multiplicative average SIC potential of the generalized Slater method. These are Kohn-Sham orbitals for LSDA and FLOs for the Jacobi and the generalized Slater methods. It is evident from the figure that the present approach, like the FLOSIC-Jacobi scheme, also produces sp -hybridized orbitals.

C. Lithium Dimer

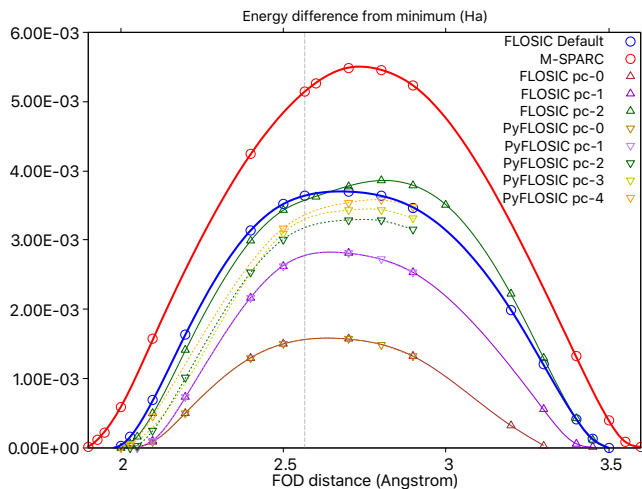


FIG. 4. Energy (E_h) as a function of FOD distance from origin for Li_2 . Energy plotted as difference from minimum energy. PyFLOSIC calculations shown as dotted lines. Atomic position shown as dashed vertical line.

We considered the Li_2 dimer as another test system. The spin-unpolarized description of Li_2 requires three FODs. By moving the outer FODs symmetrically along the bond axis, it is possible to reduce the search for optimal FOD positions to one dimension. Using this approach one finds two minima of equal energy, as shown in Fig. 3, with one corresponding to the FODs being found between the atoms and one outside the atoms. Other minima are possible with non-symmetric FOD positions, e.g. 1 outside, 1 inside.

In Fig. 4 we plot the energy as a function of the FODs' distance from the origin, shifting the energy so the minimum energy is zero. The atomic position is shown as the vertical dashed line around 2.56 Bohr from the origin. In plotting the differences with M-SPARC and the FLOSIC code using the default basis set, we found that the FOD positions in M-SPARC were pushed farther away from the atoms for both the inside and outside minima, as well as a larger energy difference at the local maximum. To determine the effect of basis set on these differences, we ran calculations utilizing the pc- n basis sets, which approach the basis set limit as n is increased from 0 to 4. We compared $n = 0 - 2$ runs with the FLOSIC and PyFLOSIC codes to verify the implementations were consistent, and performed calculations with $n = 3 - 4$ with PyFLOSIC.

Results plotted in Fig. 4 show the FOD positions and local maximum begin approaching the M-SPARC results as the basis approaches the basis set limit, but begin to converge from $n = 2 - 4$. We also tested the augmented pc-4 basis set, which adds diffuse functions, but found no difference from pc-4. The remaining difference in converged M-SPARC and FLOSIC/PyFLOSIC energies may be attributed to the different orbital densities in the core region, M-SPARC densities being smooth pseudo-densities and FLOSIC/PyFLOSIC be-

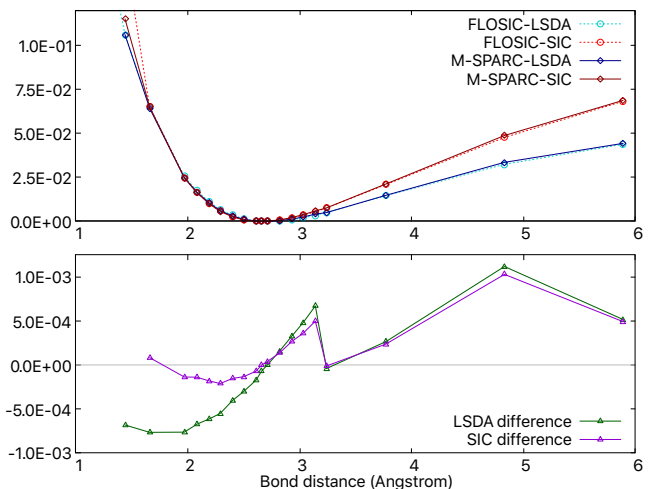


FIG. 5. Top: Energy (E_h) as a function of bond distance for Li_2 . Energy is shifted in each case so energy at equilibrium distance is zero. FODs for SIC calculations are optimized for each bond distance. Bottom: Energy difference (E_h) between FLOSIC and M-SPARC calculations at a given bond distance.

ing Gaussian all-electron.

While converged FOD positions may differ depending on potential representation, energy differences and physical observables such as equilibrium bond length should give comparable results. Figure 5 shows the energy vs. bond distance for the Li_2 molecule computed by FLOSIC and M-SPARC codes. For each bond distance, FOD forces were converged to $10^{-3} E_h/\text{Bohr}$. The results show excellent agreement over a wide range, as well as finding the same equilibrium bond length in both M-SPARC and FLOSIC code calculations. Plotting the difference between M-SPARC and FLOSIC results in Fig. 5, we see that both implementations agree to within a milli-Hartree. In the M-SPARC calculations, the results must be converged with respect to domain size and grid spacing. Errors will be larger as atoms approach the domain boundary. When the domain size is increased for the calculation around 3.2 Bohr, the error essentially vanishes. At very small bond distance, optimizing the FODs leads to cases in which they become too close and linear dependencies arise in the Löwdin-orthogonalization of the transformation matrix. In addition, pseudopotential overlap, fixed Gaussian exponents, and/or basis contraction may contribute to differences at the shortest bond distances.⁵⁸

D. Atomization Energies

The atomization energy (AE) is defined as

$$AE = \sum_i^{N_{atoms}} E_i - E_{mol} > 0,$$

where E_i is the energy of the constituent atom and E_{mol} is the energy of the molecule. We computed AEs for a set of small molecules used in the initial FLOSIC publications⁷⁰ as well

TABLE I. Atomization energies (in eV)

Molecule	FLOSIC code					M-SPARC code				Expt. ^a
	LSDA	OS-SIC	SC _{Jacobi}	SC _{AvgSIC}	SC _{0.5-AvgSIC}	LSDA	OS-SIC	SC _{AvgSIC}	SC _{0.5-AvgSIC}	
N ₂	11.54	10.25	10.24	9.92	10.06	10.99	9.64	9.60	9.60	9.76
O ₂	7.52	5.01	5.06	4.75	4.81	7.33	5.00	4.98	4.97	5.12
CO	12.92	11.28	11.07	10.52	10.94	12.68	10.95	10.90	10.91	11.11
CO ₂	20.40	15.72	15.88	14.89	15.34	20.06	15.46	15.55	15.49	16.56
C ₂ H ₂	19.90	19.27	18.83	17.83	18.72	19.68	18.79	18.69	18.71	16.86
H ₂	4.90	4.98	4.96	4.96	4.96	4.90	4.92	4.91	4.90	4.48
CH ₄	20.03	20.42	20.20	19.64	20.10	19.92	20.23	20.16	20.14	17.02
NH ₃	14.61	14.43	14.44	14.18	14.31	14.37	14.25	14.21	14.19	12.00
H ₂ O	11.55	10.68	10.67	10.49	10.57	11.42	10.65	10.62	10.61	9.51
MAE	2.33	1.28	1.16	1.11	1.20	2.10	1.16	1.14	1.14	
MARE(%)	21.4	10.2	9.3	9.4	9.8	19.3	9.2	9.0	9.0	

^a Reference [115]

as the first self-consistent implementation.¹⁰¹ FOD positions were optimized within each implementation to within $10^{-3} E_h/\text{Bohr}/\text{FOD}$. All molecular geometries and initial FOD positions were taken from Ref. [101], which were obtained using the LSDA-PW92 exchange-correlation functional and the default FLOSIC code basis set. The calculation of atomization energies requires total energies of atoms. We found that the unscaled SC_{AvgSIC} approach exhibited convergence difficulties which required relaxing the FOD optimization threshold. The lithium atom presented an additional issue in both the FLOSIC code and M-SPARC for SC_{AvgSIC} calculations. During the SCF cycle for the atom, occupation of the HOO alternates between spin-up and spin-down orbitals from iteration to iteration. The SIC energy of a run is determined from the spin-up orbital as specified at the beginning of the calculation, so the converged energy does not correctly reflect this spin change. Since this prevented us from comparing the SC calculations directly with the LSDA and OS calculations, molecules containing Li were left out of the reported average error.

The calculated AEs are shown in Table I for LSDA and OS-SIC as well as self-consistent implementations described in Sec. II C. We compare our results to the experimental atomization energies¹¹⁵ and report the mean absolute error (MAE) and mean absolute relative error (MARE) of the nine molecules. AEs for LSDA calculations are overestimated in both cases, but are slightly reduced in M-SPARC. The same can be seen in OS-SIC runs, where M-SPARC reduces the MARE from 10.2% in the FLOSIC code to 9.2% compared to experiment.

Self-consistency slightly reduces errors relative to one-shot calculations. M-SPARC SC_{AvgSIC} results show a slight improvement of 0.3 – 0.4% in the MARE compared to SC_{Jacobi} and SC_{AvgSIC} calculations using the FLOSIC code. Self-consistent calculations with the FLOSIC code differ slightly, with SC_{AvgSIC} errors slightly increased on average compared to SC_{Jacobi}. O₂, for example, increases from 1.1% to 7.3% relative error when using SC_{AvgSIC}. By scaling the SIC by 0.5 with SC_{0.5-AvgSIC}, the error improves slightly to 6.0%. In all cases, the error is much smaller compared to the LSDA error of 46.8%. In M-SPARC, the average error remains the same for SC_{AvgSIC} and scaled SC_{0.5-AvgSIC} calculations, with results

somewhat closer to experiment than FLOSIC code results.

E. Ionization potentials

The Kohn-Sham eigenvalues are not electron removal energies except for the highest occupied orbital (HOO). In exact DFT, the HOO eigenvalue equals the negative of the ionization potential.^{4,117–120} This relationship does not strictly hold for approximate density functionals used in practical applications of KS-DFT and in most DFAs the absolute value of the HOO eigenvalue substantially underestimates the first ionization potential due to SIE of the exchange-correlation potential. This can be seen easily. In this approximation the asymptotic decay of the electron density is primarily governed by the HOO density. Thus, in this limit, the weight factor $\tilde{\rho}_i/\rho$ approaches unity. Therefore, correcting for self-interaction results in the $-1/r$ asymptotic behavior of the exchange-correlation potential and provides a significant improvement in the HOO eigenvalue.

In Table II, we show the HOO eigenvalues obtained by the present real-space M-SPARC and existing Gaussian-based FLOSIC codes. We compare the computed HOO eigenvalues against the experimental ionization potentials (IPs)¹¹⁶ and report MAEs and MAREs for the set. The LSDA M-SPARC and FLOSIC code eigenvalues agree well, with MAE of 4.55 eV relative to experiment. The application of SIC using the SC_{AvgSIC} method reduces the MAE from 4.55 eV to 2.42 eV for the FLOSIC code and from 4.55 eV to 2.24 eV for M-SPARC. Although the HOO eigenvalues in the SC_{AvgSIC} method are improved with respect to LSDA, they are overestimated with respect to experimental eigenvalues. This overestimation can be mitigated by scaling down the \tilde{v}_{SIC}^σ potential. The HOO eigenvalues obtained by scaling down the \tilde{v}_{SIC}^σ potential by 0.5 show clear improvements with further decreases in MAE to 1.14 eV for the FLOSIC code and to 1.21 eV for M-SPARC.

TABLE II. Ionization potentials (in eV)

Molecule	FLOSIC code				M-SPARC code			Expt. ^a
	LSDA	SC _{Jacobi}	SC _{AvgSIC}	SC _{0.5-AvgSIC}	LSDA	SC _{AvgSIC}	SC _{0.5-AvgSIC}	
N ₂	10.43	17.79	18.16	14.22	10.44	17.75	14.05	15.58
O ₂	7.05	15.95	16.68	11.74	7.14	16.47	11.73	12.30
CO	9.15	15.70	16.20	12.60	9.16	15.85	12.46	14.01
CO ₂	9.31	16.07	17.04	13.11	9.33	16.73	12.99	13.78
C ₂ H ₂	7.34	12.59	13.48	10.35	7.34	13.29	10.28	11.49
LiF	6.26	13.77	14.44	10.19	6.32	14.42	10.26	11.30
H ₂	10.22	16.78	16.80	13.47	10.03	16.45	13.20	15.43
Li ₂	3.23	5.48	5.89	4.51	3.16	5.84	4.45	5.11
CH ₄	9.43	15.90	16.00	12.67	9.44	16.04	12.70	13.60
NH ₃	6.27	12.61	12.96	9.54	6.28	12.90	9.53	10.82
H ₂ O	7.33	14.87	14.99	11.09	7.37	14.95	11.09	12.62
MAE	4.55	1.95	2.42	1.14	4.55	2.24	1.21	
MARE(%)	37.1	15.6	19.7	9.4	37.2	18.4	9.9	

^a Reference [116]

F. Barrier heights of chemical reactions

Finally, we test the present implementation using the BH6 database of barrier heights in chemical reactions. BH6 is a representative subset of the BH24 set.¹²¹ The reactions included in BH6 are: $\text{OH} + \text{CH}_4 \rightarrow \text{CH}_3 + \text{H}_2\text{O}$, $\text{H} + \text{OH} \rightarrow \text{H}_2 + \text{O}$, and $\text{H} + \text{H}_2\text{S} \rightarrow \text{H}_2 + \text{HS}$. Total energies at the left hand side, the right hand side, and the saddle point of these chemical reactions were calculated, and the barrier heights of the forward (f) and reverse (r) reactions were obtained by taking the relevant energy differences. The geometries used are same as those provided in Ref. [121]. The reference values are from Ref. [122]. The results for the methods considered are summarized in Table III. The local (and also semi-local) DFAs underestimate barrier heights¹⁴ by giving transition state energies that are too low compared to the reactant and product energies. Accurate description of transition states require full nonlocality in the exchange-correlation potential that local (and semi-local) approximations lack. The present SC_{AvgSIC} scheme further improves over SC_{Jacobi}. The MAE in barrier heights in the SC_{AvgSIC} implementation is 2.8 kcal/mol vs. 4.9 kcal/mol for the SC_{Jacobi} method, corresponding to a 14.1% improvement in MARE.

V. CONCLUSION

We presented a formulation and implementation of the FLOSIC self-interaction correction in real space. The real-space formulation allows rigorous, systematic convergence for all atomic species and configurations. The present M-SPARC based implementation demonstrated the feasibility and accuracy of the real-space formulation. Self-consistency in the present work was introduced using a generalized Slater statistical average SIC potential.

We verified our M-SPARC based real-space implementation by computing atomization energies and ionization potentials of selected molecules and comparing to those obtained by the established Gaussian-based FLOSIC and

PyFLOSIC codes. We compared results for LSDA and non-self-consistent as well as self-consistent FLOSIC calculations. The results obtained with the M-SPARC code show good agreement with those obtained by the Gaussian-based FLOSIC code, with M-SPARC results somewhat closer to experiment for the systems considered. The application of SIC with Slater-averaged SIC potentials showed improvement in HOOs over LSDA. We found that scaling down the SIC potential by a factor of 0.5 gives comparable or improved results compared to the all-electron Gaussian-based FLOSIC code implementation. The MAE in computed ionization potentials with respect to experiment was found to be 2.24 eV and decreases to 1.21 eV when the SIC potential is scaled down by 0.5. We also found that the barrier heights obtained using the present SC_{AvgSIC} scheme are further improved over the SC_{Jacobi} barrier heights. Our initial results indicate that the real-space formulation provides an accurate and systematically improvable approach for FLOSIC calculations in the Slater-average form. Future work will include implementation in the large-scale parallel SPARC code and extension to a full OEP formulation.

VI. ACKNOWLEDGEMENTS

C.M.D., T. B., and R. R. Z. acknowledge discussions with Dr. Yoh Yamamoto and thank Prof. Koblak Jackson for reading the manuscript. This material is based upon work supported by the U.S. Department of Energy, Office of Science, Office of Workforce Development for Teachers and Scientists, Office of Science Graduate Student Research (SCGSR) program. The SCGSR program is administered by the Oak Ridge Institute for Science and Education (ORISE) for the DOE. ORISE is managed by ORAU under contract number DE-SC0014664. C.M.D., T.B. and R.R.Z. acknowledge support by the US Department of Energy, Office of Science, Office of Basic Energy Sciences, as part of the Computational Chemical Sciences Program under Award No. DE-SC0018331. This work was performed in part under the auspices of the U.S. De-

TABLE III. Barrier heights in kcal/mol of the forward (f) and reverse (r) chemical reactions belonging to the BH6 database. Signed errors are shown.

Reaction	Barrier	FLOSIC code		M-SPARC code			Ref. ^b
		LSDA	SC _{Jacobi} ^a	LSDA	OS-SIC	SC _{AvgSIC}	
OH + CH ₄ → CH ₃ + H ₂ O	f	-23.6	-2.2	-22.9	1.0	1.0	6.7
	r	-17.4	-12.5	-17.0	-6.5	-6.6	19.6
H + OH → H ₂ + O	f	-11.8	-1.1	-13.1	-1.6	-0.1	10.7
	r	-25.3	-4.8	-24.8	-0.5	0.9	13.1
H + H ₂ S → H ₂ + HS	f	-10.3	-1.7	-10.0	-0.9	-1.0	3.6
	r	-17.2	-7.0	-16.5	-3.9	-6.0	17.3
MAE		17.6	4.9	17.4	2.4	2.8	
MARE		188.3%	38.5%	185.7%	19.0%	24.4%	

^a Reference [16]^b Reference [122]

partment of Energy by Lawrence Livermore National Laboratory under Contract DE-AC52-07NA27344. P.S. and Q.X. acknowledge support by the grant DE-SC0019410 funded by the U.S. Department of Energy, Office of Science. All opinions expressed in this paper are the authors' and do not necessarily reflect the policies and views of DOE, ORAU, or ORISE.

VII. DATA AVAILABILITY

The data that support the findings of this study are available from the corresponding author upon reasonable request.

VIII. REFERENCES

- R. O. Jones, "Density functional theory: Its origins, rise to prominence, and future," *Rev. Mod. Phys.* **87**, 897 (2015).
- J. P. Perdew and K. Schmidt, "Jacob's ladder of density functional approximations for the exchange-correlation energy," in *AIP Conference Proceedings*, Vol. 577 (AIP, 2001) pp. 1–20.
- M. A. Marques, M. J. Oliveira, and T. Burnus, "Libxc: A library of exchange and correlation functionals for density functional theory," *Computer Physics Communications* **183**, 2272–2281 (2012).
- J. P. Perdew, R. G. Parr, M. Levy, and J. L. Balduz Jr, "Density-functional theory for fractional particle number: derivative discontinuities of the energy," *Phys. Rev. Lett.* **49**, 1691 (1982).
- T. Tsuneda and K. Hirao, "Parameter-free exchange functional," *Physical Review B* **62**, 15527 (2000).
- W. Kohn and L. Sham, "Self-consistent equations including exchange and correlation effects," *Phys. Rev.* **140**, A1133–A1138 (1965).
- J. P. Perdew and A. Zunger, "Self-interaction correction to density-functional approximations for many-electron systems," *Phys. Rev. B* **23**, 5048–5079 (1981).
- S. Patchkovskii, J. Autschbach, and T. Ziegler, "Curing difficult cases in magnetic properties prediction with self-interaction corrected density functional theory," *J. Chem. Phys.* **115**, 26–42 (2001), <https://doi.org/10.1063/1.1370527>.
- I. Lindgren, "A statistical exchange approximation for localized electrons," *Int. J. Quantum Chem.* **5**, 411–420 (1971).
- J. Perdew, "Orbital functional for exchange and correlation: self-interaction correction to the local density approximation," *Chem. Phys. Lett.* **64**, 127–130 (1979).
- M. S. Gopinathan, "Improved approximate representation of the Hartree-Fock potential in atoms," *Phys. Rev. A* **15**, 2135–2142 (1977).
- O. Gunnarsson and R. O. Jones, "Self-interaction corrections in the density functional formalism," *Solid State Commun.* **37**, 249–252 (1981).
- U. Lundin and O. Eriksson, "Novel method of self-interaction corrections in density functional calculations," *Int. J. Quantum Chem.* **81**, 247–252 (2001).
- O. A. Vydrov, G. E. Scuseria, J. P. Perdew, A. Ruzsinszky, and G. I. Csonka, "Scaling down the Perdew-Zunger self-interaction correction in many-electron regions," *J. Chem. Phys.* **124**, 094108 (2006), <https://doi.org/10.1063/1.2176608>.
- Y. Yamamoto, S. Romero, T. Baruah, and R. R. Zope, "Improvements in the orbitalwise scaling down of perdew-zunger self-interaction correction in many-electron regions," *The Journal of Chemical Physics* **152**, 174112 (2020), <https://doi.org/10.1063/5.0004738>.
- R. R. Zope, Y. Yamamoto, C. M. Diaz, T. Baruah, J. E. Peralta, K. A. Jackson, B. Santra, and J. P. Perdew, "A step in the direction of resolving the paradox of Perdew-Zunger self-interaction correction," *J. Chem. Phys.* **151**, 214108 (2019), <https://doi.org/10.1063/1.5129533>.
- R. A. Heaton, J. G. Harrison, and C. C. Lin, "Self-interaction correction for density-functional theory of electronic energy bands of solids," *Phys. Rev. B* **28**, 5992–6007 (1983).
- M. R. Pederson, R. A. Heaton, and C. C. Lin, "Local-density Hartree-Fock theory of electronic states of molecules with self-interaction correction," *J. Chem. Phys.* **80**, 1972–1975 (1984), <https://doi.org/10.1063/1.446959>.
- M. R. Pederson, R. A. Heaton, and C. C. Lin, "Density-functional theory with self-interaction correction: Application to the lithium molecule," *J. Chem. Phys.* **82**, 2688–2699 (1985), <https://doi.org/10.1063/1.448266>.
- J. Garza, J. A. Nichols, and D. A. Dixon, "The optimized effective potential and the self-interaction correction in density functional theory: Application to molecules," *J. Chem. Phys.* **112**, 7880–7890 (2000), <https://doi.org/10.1063/1.481421>.
- J. Garza, R. Vargas, J. A. Nichols, and D. A. Dixon, "Orbital energy analysis with respect to LDA and self-interaction corrected exchange-only potentials," *J. Chem. Phys.* **114**, 639–651 (2001), <https://aip.scitation.org/doi/pdf/10.1063/1.1327269>.
- M. K. Harbola, "Theoretical investigation of the polarizability of small metal clusters," *Solid State Commun.* **98**, 629–632 (1996).
- S. Patchkovskii and T. Ziegler, "Improving "difficult" reaction barriers with self-interaction corrected density functional theory," *J. Chem. Phys.* **116**, 7806–7813 (2002), <https://doi.org/10.1063/1.1468640>.
- S. Patchkovskii and T. Ziegler, "Phosphorus NMR chemical shifts with self-interaction free, gradient-corrected DFT," *J. Phys. Chem. A* **106**, 1088–1099 (2002), <https://doi.org/10.1021/jp014184v>.
- S. Goedecker and C. J. Umrigar, "Critical assessment of the self-interaction-corrected-local-density-functional method and its algorithmic implementation," *Phys. Rev. A* **55**, 1765–1771 (1997).
- V. Polo, E. Kraka, and D. Cremer, "Electron correlation and the self-interaction error of density functional theory," *Mol. Phys.* **100**, 1771–1790 (2002), <https://doi.org/10.1080/00268970110111788>.
- V. Polo, J. Gräfenstein, E. Kraka, and D. Cremer, "Long-range and short-range coulomb correlation effects as simulated by Hartree-Fock, local density approximation, and generalized gradient approximation exchange functionals," *Theor. Chim. Acta* **109**, 22–35 (2003).

- ²⁸J. Gräfenstein, E. Kraka, and D. Cremer, "The impact of the self-interaction error on the density functional theory description of dissociating radical cations: Ionic and covalent dissociation limits," *J. Chem. Phys.* **120**, 524–539 (2004), <https://doi.org/10.1063/1.1630017>.
- ²⁹J. Gräfenstein, E. Kraka, and D. Cremer, "Effect of the self-interaction error for three-electron bonds: On the development of new exchange-correlation functionals," *Phys. Chem. Chem. Phys.* **6**, 1096–1112 (2004).
- ³⁰O. A. Vydrov and G. E. Scuseria, "Effect of the Perdew-Zunger self-interaction correction on the thermochemical performance of approximate density functionals," *J. Chem. Phys.* **121**, 8187–8193 (2004), <https://aip.scitation.org/doi/pdf/10.1063/1.1794633>.
- ³¹O. A. Vydrov and G. E. Scuseria, "Ionization potentials and electron affinities in the Perdew-Zunger self-interaction corrected density-functional theory," *J. Chem. Phys.* **122**, 184107 (2005), <https://doi.org/10.1063/1.1897378>.
- ³²R. R. Zope, M. K. Harbola, and R. K. Pathak, "Atomic Compton profiles within different exchange-only theories," *Eur. Phys. J. D* **7**, 151–155 (1999).
- ³³O. A. Vydrov and G. E. Scuseria, "A simple method to selectively scale down the self-interaction correction," *J. Chem. Phys.* **124**, 191101 (2006), <https://doi.org/10.1063/1.2204599>.
- ³⁴T. Tsuneda, M. Kamiya, and K. Hirao, "Regional self-interaction correction of density functional theory," *J. Chem. Phys.* **24**, 1592–1598 (2003), <https://onlinelibrary.wiley.com/doi/pdf/10.1002/jcc.10279>.
- ³⁵J. B. Krieger, Y. Li, and G. J. Iafrate, "Construction and application of an accurate local spin-polarized Kohn-Sham potential with integer discontinuity: Exchange-only theory," *Phys. Rev. A* **45**, 101–126 (1992).
- ³⁶J. B. Krieger, Y. Li, and G. J. Iafrate, "Systematic approximations to the optimized effective potential: Application to orbital-density-functional theory," *Phys. Rev. A* **46**, 5453–5458 (1992).
- ³⁷Y. Li, J. B. Krieger, and G. J. Iafrate, "Self-consistent calculations of atomic properties using self-interaction-free exchange-only Kohn-Sham potentials," *Phys. Rev. A* **47**, 165–181 (1993).
- ³⁸S. Lehtola, M. Head-Gordon, and H. Jónsson, "Complex orbitals, multiple local minima, and symmetry breaking in Perdew-Zunger self-interaction corrected density functional theory calculations," *J. Chem. Theory Comput.* **12**, 3195–3207 (2016).
- ³⁹G. I. Csonka and B. G. Johnson, "Inclusion of exact exchange for self-interaction corrected H3 density functional potential energy surface," *Theor. Chim. Acta* **99**, 158–165 (1998).
- ⁴⁰L. Petit, A. Svane, M. Lüders, Z. Szotek, G. Vaitheeswaran, V. Kanchana, and W. Temmerman, "Phase transitions in rare earth tellurides under pressure," *J. Phys. Cond. Matter* **26**, 274213 (2014).
- ⁴¹S. Kümmel and L. Kronik, "Orbital-dependent density functionals: Theory and applications," *Rev. Mod. Phys.* **80**, 3 (2008).
- ⁴²T. Schmidt, E. Kraisler, L. Kronik, and S. Kümmel, "One-electron self-interaction and the asymptotics of the Kohn-Sham potential: an impaired relation," *Phys. Chem. Chem. Phys.* **16**, 14357–14367 (2014).
- ⁴³D.-y. Kao, M. Pederson, T. Hahn, T. Baruah, S. Liebing, and J. Kortus, "The role of self-interaction corrections, vibrations, and spin-orbit in determining the ground spin state in a simple heme," *Magnetochemistry* **3**, 31 (2017).
- ⁴⁴S. Schwalbe, T. Hahn, S. Liebing, K. Trepte, and J. Kortus, "Fermi-Löwdin orbital self-interaction corrected density functional theory: Ionization potentials and enthalpies of formation," *J. Comp. Chem.* **39**, 2463–2471 (2018), <https://onlinelibrary.wiley.com/doi/pdf/10.1002/jcc.25586>.
- ⁴⁵H. Jónsson, K. Tsemekhman, and E. J. Bylaska, "Accurate self-interaction correction to semilocal density functionals," in *Abstracts of Papers of the American Chemical Society*, Vol. 233 (American Chemical Society 1155 16TH ST, NW, Washington, DC 20036 USA, 2007) pp. 120–120.
- ⁴⁶M. M. Rieger and P. Vogl, "Self-interaction corrections in semiconductors," *Phys. Rev. B* **52**, 16567 (1995).
- ⁴⁷W. Temmerman, A. Svane, Z. Szotek, H. Winter, and S. Beiden, "On the implementation of the self-interaction corrected local spin density approximation for d- and f-electron systems," in *Electronic Structure and Physical Properties of Solids* (Springer, 1999) pp. 286–312.
- ⁴⁸M. Daene, M. Lueders, A. Ernst, D. Ködderitzsch, W. M. Temmerman, Z. Szotek, and W. Hergert, "Self-interaction correction in multiple scattering theory: application to transition metal oxides," *J. Phys. Cond. Matter* **21**, 045604 (2009).
- ⁴⁹Z. Szotek, W. Temmerman, and H. Winter, "Self-interaction correction of localized bands within the LMTO-ASA band structure method," *Physica B: Condensed Matter* **172**, 19–25 (1991).
- ⁵⁰J. Messud, P. M. Dinh, P.-G. Reinhard, and E. Suraud, "Time-dependent density-functional theory with a self-interaction correction," *Phys. Rev. Lett.* **101**, 096404 (2008).
- ⁵¹J. Messud, P. M. Dinh, P.-G. Reinhard, and E. Suraud, "Improved Slater approximation to SIC-OEP," *Chem. Phys. Lett.* **461**, 316–320 (2008).
- ⁵²M. Lundberg and P. E. M. Siegbahn, "Quantifying the effects of the self-interaction error in DFT: When do the delocalized states appear?" *J. Chem. Phys.* **122**, 224103 (2005), <https://doi.org/10.1063/1.1926277>.
- ⁵³T. Körzdörfer, M. Mundt, and S. Kümmel, "Electrical response of molecular systems: the power of self-interaction corrected Kohn-Sham theory," *Phys. Rev. Lett.* **100**, 133004 (2008).
- ⁵⁴T. Körzdörfer, S. Kümmel, and M. Mundt, "Self-interaction correction and the optimized effective potential," *Journal of Chemical Physics* **129** (2008), 10.1063/1.2944272.
- ⁵⁵I. Ciofini, C. Adamo, and H. Chermette, "Self-interaction error in density functional theory: a mean-field correction for molecules and large systems," *Chem. Phys.* **309**, 67–76 (2005).
- ⁵⁶T. Baruah, R. R. Zope, A. Kshirsagar, and R. K. Pathak, "Positron binding: A positron-density viewpoint," *Phys. Rev. A* **50**, 2191–2196 (1994).
- ⁵⁷A. I. Johnson, K. P. K. Withanage, K. Sharkas, Y. Yamamoto, T. Baruah, R. R. Zope, J. E. Peralta, and K. A. Jackson, "The effect of self-interaction error on electrostatic dipoles calculated using density functional theory," *J. Chem. Phys.* **151**, 174106 (2019), <https://doi.org/10.1063/1.5125205>.
- ⁵⁸J. Vargas, P. Uföndu, T. Baruah, Y. Yamamoto, K. A. Jackson, and R. R. Zope, "Importance of self-interaction-error removal in density functional calculations on water cluster anions," *Phys. Chem. Chem. Phys.*, – (2020).
- ⁵⁹K. Trepte, S. Schwalbe, T. Hahn, J. Kortus, D.-Y. Kao, Y. Yamamoto, T. Baruah, R. R. Zope, K. P. K. Withanage, J. E. Peralta, and K. A. Jackson, "Analytic atomic gradients in the Fermi-Löwdin orbital self-interaction correction," *J. Comput. Chem.* **40**, 820–825 (2019), <https://onlinelibrary.wiley.com/doi/pdf/10.1002/jcc.25767>.
- ⁶⁰K. P. K. Withanage, K. Trepte, J. E. Peralta, T. Baruah, R. Zope, and K. A. Jackson, "On the question of the total energy in the Fermi-Löwdin orbital self-interaction correction method," *J. Chem. Theory Comput.* **14**, 4122–4128 (2018), pMID: 29986131, <https://doi.org/10.1021/acs.jctc.8b00344>.
- ⁶¹M. R. Pederson, T. Baruah, D.-y. Kao, and L. Basurto, "Self-interaction corrections applied to Mg-porphyrin, C₆₀, and pentacene molecules," *J. Chem. Phys.* **144**, 164117 (2016), <https://doi.org/10.1063/1.4947042>.
- ⁶²S. Schwalbe, L. Fiedler, T. Hahn, K. Trepte, J. Kraus, and J. Kortus, "PyFLOSIC - python based Fermi-Löwdin orbital self-interaction correction," (2019), arXiv:1905.02631 [physics.comp-ph].
- ⁶³D.-y. Kao, K. Withanage, T. Hahn, J. Batool, J. Kortus, and K. Jackson, "Self-consistent self-interaction corrected density functional theory calculations for atoms using Fermi-Löwdin orbitals: Optimized Fermi-orbital descriptors for li-kr," *J. Chem. Phys.* **147**, 164107 (2017), <https://doi.org/10.1063/1.4996498>.
- ⁶⁴R. P. Joshi, K. Trepte, K. P. K. Withanage, K. Sharkas, Y. Yamamoto, L. Basurto, R. R. Zope, T. Baruah, K. A. Jackson, and J. E. Peralta, "Fermi-Löwdin orbital self-interaction correction to magnetic exchange couplings," *J. Chem. Phys.* **149**, 164101 (2018).
- ⁶⁵K. Sharkas, L. Li, K. Trepte, K. P. K. Withanage, R. P. Joshi, R. R. Zope, T. Baruah, J. K. Johnson, K. A. Jackson, and J. E. Peralta, "Shrinking self-interaction errors with the Fermi-Löwdin orbital self-interaction-corrected density functional approximation," *J. Phys. Chem. A* **122**, 9307–9315 (2018), pMID: 30412407.
- ⁶⁶K. A. Jackson, J. E. Peralta, R. P. Joshi, K. P. Withanage, K. Trepte, K. Sharkas, and A. I. Johnson, "Towards efficient density functional theory calculations without self-interaction: The Fermi-Löwdin orbital self-interaction correction," *J. Phys. Conf. Ser.* **1290**, 012002 (2019).
- ⁶⁷K. Sharkas, K. Wagle, B. Santra, S. Akter, R. R. Zope, T. Baruah, K. A. Jackson, J. P. Perdew, and J. E. Peralta, "Self-interaction error overbinds water clusters but cancels in structural energy differences," *Proceedings of the National Academy of Sciences* **117**, 11283–11288 (2020), <https://www.pnas.org/content/117/21/11283.full.pdf>.
- ⁶⁸J. M. Foster and S. F. Boys, "Canonical configurational interaction procedure," *Reviews of Modern Physics* **32**, 300–302 (1960).

- ⁶⁹J. Pipek and P. G. Mezey, "A fast intrinsic localization procedure applicable for ab initio and semiempirical linear combination of atomic orbital wave functions," *The Journal of Chemical Physics* **90**, 4916–4926 (1989).
- ⁷⁰M. R. Pederson, A. Ruzsinszky, and J. P. Perdew, "Communication: Self-interaction correction with unitary invariance in density functional theory," *J. Chem. Phys.* **140**, 121103 (2014).
- ⁷¹J. M. Leonard and W. L. Luken, "Quadratically convergent calculation of localized molecular orbitals," *Theor. Chem. Acc.* **62**, 107–132 (1982).
- ⁷²W. L. Luken and D. N. Beratan, "Localized orbitals and the Fermi hole," *Theor. Chem. Acc.* **61**, 265–281 (1982).
- ⁷³W. L. Luken and J. C. Culberson, "Localized orbitals based on the Fermi hole," *Theor. Chem. Acc.* **66**, 279–293 (1984).
- ⁷⁴M. R. Pederson, "Fermi orbital derivatives in self-interaction corrected density functional theory: Applications to closed shell atoms," *J. Chem. Phys.* **142**, 064112 (2015), <https://doi.org/10.1063/1.4907592>.
- ⁷⁵M. R. Pederson and T. Baruah, "Chapter eight - self-interaction corrections within the Fermi-orbital-based formalism," in *Advances In Atomic, Molecular, and Optical Physics*, Vol. 64 (Academic Press, 2015) pp. 153–180.
- ⁷⁶K. P. K. Withanage, S. Akter, C. Shahi, R. P. Joshi, C. Diaz, Y. Yamamoto, R. Zope, T. Baruah, J. P. Perdew, J. E. Peralta, and K. A. Jackson, "Self-interaction-free electric dipole polarizabilities for atoms and their ions using the Fermi-Löwdin self-interaction correction," *Phys. Rev. A* **100**, 012505 (2019).
- ⁷⁷C. Shahi, P. Bhattarai, K. Wagle, B. Santra, S. Schwalbe, T. Hahn, J. Kortus, K. A. Jackson, J. E. Peralta, K. Trepte, S. Lehtola, N. K. Nepal, H. Myrneni, B. Neupane, S. Adhikari, A. Ruzsinszky, Y. Yamamoto, T. Baruah, R. R. Zope, and J. P. Perdew, "Stretched or noded orbital densities and self-interaction correction in density functional theory," *J. Chem. Phys.* **150**, 174102 (2019).
- ⁷⁸Y. Yamamoto, C. M. Diaz, L. Basurto, K. A. Jackson, T. Baruah, and R. R. Zope, "Fermi-Löwdin orbital self-interaction correction using the strongly constrained and appropriately normed meta-GGA functional," *J. Chem. Phys.* **151**, 154105 (2019), AE6 result extracted from the data in this publication., <https://doi.org/10.1063/1.5120532>.
- ⁷⁹M. R. Pederson and T. Baruah, "Single Hamiltonian for self-interaction corrected DFT with Fermi-Löwdin orbitals," Unpublished.
- ⁸⁰T. Schmidt, E. Kraissler, A. Makmal, L. Kronik, and S. Kümmel, "A self-interaction-free local hybrid functional: Accurate binding energies vis-à-vis accurate ionization potentials from Kohn-Sham eigenvalues," *Journal of Chemical Physics* **140**, 18A510 (2014), arXiv:1405.5809.
- ⁸¹Q. Xu, A. Sharma, and P. Suryanarayana, "M-SPARC: Matlab-Simulation Package for Ab-initio Real-space Calculations," *SoftwareX* **11**, 100423 (2020).
- ⁸²S. Ghosh and P. Suryanarayana, "SPARC: Accurate and efficient finite-difference formulation and parallel implementation of density functional theory: Extended systems," *Computer Physics Communications* **216**, 109–125 (2017).
- ⁸³S. Ghosh and P. Suryanarayana, "SPARC: Accurate and efficient finite-difference formulation and parallel implementation of density functional theory: Isolated clusters," *Computer Physics Communications* **212**, 189–204 (2017).
- ⁸⁴Q. Xu, A. Sharma, B. Comer, H. Huang, E. Chow, A. J. Medford, J. E. Pask, and P. Suryanarayana, "Sparc: Simulation package for ab-initio real-space calculations," arXiv preprint arXiv:2005.10431 (2020).
- ⁸⁵R. Martin, *Electronic Structure: Basic theory and practical methods* (Cambridge University Press, 2004).
- ⁸⁶J. Pask and P. Sterne, "Real-space formulation of the electrostatic potential and total energy of solids," *Phys. Rev. B* **71**, 113101 (2005).
- ⁸⁷P. Suryanarayana and D. Phanish, "Augmented Lagrangian formulation of orbital-free density functional theory," *Journal of Computational Physics* **275**, 524–538 (2014).
- ⁸⁸S. Ghosh and P. Suryanarayana, "Higher-order finite-difference formulation of periodic orbital-free density functional theory," *Journal of Computational Physics* **307**, 634–652 (2016).
- ⁸⁹D. Alfe, "Ab initio molecular dynamics, a simple algorithm for charge extrapolation," *Computer Physics Communications* **118**, 31–33 (1999).
- ⁹⁰P. P. Pratapa and P. Suryanarayana, "Restarted Pulay mixing for efficient and robust acceleration of fixed-point iterations," *Chemical Physics Letters* **635**, 69–74 (2015).
- ⁹¹A. S. Banerjee, P. Suryanarayana, and J. E. Pask, "Periodic Pulay method for robust and efficient convergence acceleration of self-consistent field iterations," *Chemical Physics Letters* **647**, 31–35 (2016).
- ⁹²S. Kumar, Q. Xu, and P. Suryanarayana, "On preconditioning the self-consistent field iteration in real-space density functional theory," *Chemical Physics Letters* **739**, 136983 (2020).
- ⁹³Y. Zhou, Y. Saad, M. L. Tiago, and J. R. Chelikowsky, "Self-consistent-field calculations using Chebyshev-filtered subspace iteration," *Journal of Computational Physics* **219**, 172–184 (2006).
- ⁹⁴Y. Zhou, Y. Saad, M. L. Tiago, and J. R. Chelikowsky, "Parallel self-consistent-field calculations via Chebyshev-filtered subspace acceleration," *Physical Review E* **74**, 066704 (2006).
- ⁹⁵Y. Zhou, J. R. Chelikowsky, and Y. Saad, "Chebyshev-filtered subspace iteration method free of sparse diagonalization for solving the Kohn–Sham equation," *Journal of Computational Physics* **274**, 770–782 (2014).
- ⁹⁶A. Sharma and P. Suryanarayana, "On real-space density functional theory for non-orthogonal crystal systems: Kronecker product formulation of the kinetic energy operator," *Chemical Physics Letters* **700**, 156–162 (2018).
- ⁹⁷P. P. Pratapa, P. Suryanarayana, and J. E. Pask, "Anderson acceleration of the Jacobi iterative method: An efficient alternative to Krylov methods for large, sparse linear systems," *Journal of Computational Physics* **306**, 43–54 (2016).
- ⁹⁸P. Suryanarayana, P. P. Pratapa, and J. E. Pask, "Alternating Anderson–Richardson method: An efficient alternative to preconditioned Krylov methods for large, sparse linear systems," *Computer Physics Communications* **234**, 278–285 (2019).
- ⁹⁹W. R. Burdick, Y. Saad, L. Kronik, I. Vasiliev, M. Jain, and J. R. Chelikowsky, "Parallel implementation of time-dependent density functional theory," *Computer Physics Communications* **156**, 22–42 (2003).
- ¹⁰⁰A. Natan, A. Benjamini, D. Naveh, L. Kronik, M. L. Tiago, S. P. Beckman, and J. R. Chelikowsky, "Real-space pseudopotential method for first principles calculations of general periodic and partially periodic systems," *Physical Review B* **78**, 075109 (2008).
- ¹⁰¹Z. H. Yang, M. R. Pederson, and J. P. Perdew, "Full self-consistency in the Fermi-orbital self-interaction correction," *Phys. Rev. A* **95**, 052505 (2017).
- ¹⁰²Q. Xu, P. Suryanarayana, and J. E. Pask, "Discrete discontinuous basis projection method for large-scale electronic structure calculations," *The Journal of Chemical Physics* **149**, 094104 (2018).
- ¹⁰³J. C. Slater, "A simplification of the Hartree-Fock method," *Physical Review* (1951), 10.1103/PhysRev.81.385.
- ¹⁰⁴J. Messud, P. M. Dinh, P.-G. Reinhard, and E. Suraud, "The generalized SIC-OEP formalism and the generalized SIC-Slater approximation (stationary and time-dependent cases)," *Annalen der Physik* **523**, 270–290 (2011).
- ¹⁰⁵M. R. Pederson and J. P. Perdew, "5 scientific highlight of the month self-interaction correction in density functional theory: The road less traveled," *Psi-k Newsletter* **109**, 77 (2012).
- ¹⁰⁶S. Klüpfel, P. Klüpfel, and H. Jónsson, "The effect of the Perdew-Zunger self-interaction correction to density functionals on the energetics of small molecules," *J. Chem. Phys.* **137**, 124102 (2012).
- ¹⁰⁷D. R. Hamann, "Optimized norm-conserving vanderbilt pseudopotentials," *Phys. Rev. B* **88**, 085117 (2013).
- ¹⁰⁸J. P. Perdew, K. Burke, and M. Ernzerhof, "Generalized gradient approximation made simple," *Phys. Rev. Lett.* **77**, 3865–3868 (1996).
- ¹⁰⁹M. Schlipf and F. Gygi, "Optimization algorithm for the generation of oncv pseudopotentials," *Computer Physics Communications* **196**, 36–44 (2015).
- ¹¹⁰M. R. Pederson and K. A. Jackson, "Variational mesh for quantum-mechanical simulations," *Phys. Rev. B* **41**, 7453–7461 (1990).
- ¹¹¹K. Jackson and M. R. Pederson, "Accurate forces in a local-orbital approach to the local-density approximation," *Physical Review B* **42**, 3276–3281 (1990).
- ¹¹²S. Schwalbe, L. Fiedler, T. Hahn, K. Trepte, J. Kraus, and J. Kortus, "PyFLOSIC - Python based Fermi-Löwdin orbital self-interaction correction," (2019), arXiv:1905.02631.
- ¹¹³Q. Sun, T. C. Berkelbach, N. S. Blunt, G. H. Booth, S. Guo, Z. Li, J. Liu, J. D. McClain, E. R. Sayfutyarova, S. Sharma, *et al.*, "Pyscf: the python-based simulations of chemistry framework," *Wiley Interdisciplinary Reviews: Computational Molecular Science* **8**, e1340 (2018).
- ¹¹⁴F. Jensen, "Polarization consistent basis sets: Principles," *Journal of Chemical Physics* (2001), 10.1063/1.1413524.

- ¹¹⁵National Institute of Standards and Technology, NIST Computational Chemistry Comparison and Benchmark Database NIST Standard Reference Database Number 101 Release 19, April 2018, Editor: Russell D. Johnson III <http://cccbdb.nist.gov/> DOI:10.18434/T47C7Z.
- ¹¹⁶G. Zhang and C. B. Musgrave, "Comparison of DFT methods for molecular orbital eigenvalue calculations," *Journal of Physical Chemistry A* (2007), 10.1021/jp061633o.
- ¹¹⁷M. Levy, J. P. Perdew, and V. Sahni, "Exact differential equation for the density and ionization energy of a many-particle system," *Phys. Rev. A* **30**, 2745–2748 (1984).
- ¹¹⁸C.-O. Almbladh and U. von Barth, "Exact results for the charge and spin densities, exchange-correlation potentials, and density-functional eigenvalues," *Phys. Rev. B* **31**, 3231 (1985).
- ¹¹⁹J. P. Perdew and M. Levy, "Comment on "Significance of the highest occupied Kohn-Sham eigenvalue"," *Phys. Rev. B* **56**, 16021 (1997).
- ¹²⁰M. K. Harbola, "Relationship between the highest occupied Kohn-Sham orbital eigenvalue and ionization energy," *Phys. Rev. B* **60**, 4545–4550 (1999).
- ¹²¹J. Zheng, Y. Zhao, and D. G. Truhlar, "Representative benchmark suites for barrier heights of diverse reaction types and assessment of electronic structure methods for thermochemical kinetics," *J. Chem. Theory Comput.* **3**, 569–582 (2007), PMID: 26637036, <https://doi.org/10.1021/ct600281g>.
- ¹²²B. J. Lynch and D. G. Truhlar, "Small representative benchmarks for thermochemical calculations," *J. Phys. Chem. A* **107**, 8996–8999 (2003), <https://doi.org/10.1021/jp035287b>.